

Hyperbolic Metamaterial Nano-Resonators Make Poor Single Photon Sources

Simon Axelrod,¹ Mohsen Kamandar Dezfouli,¹ Herman M. K. Wong,² Amr S. Helmy,² and Stephen Hughes^{1,*}

¹*Department of Physics, Engineering Physics and Astronomy,
Queen's University, Kingston, Canada, K7L 3N6*

²*Photonics Group, Edward S. Rogers Sr. Department of Electrical and Computer Engineering,
University of Toronto, Toronto, Canada, M5S 3H6*

We study the optical properties of quantum dipole emitters coupled to hyperbolic metamaterial nano-resonators using a semi-analytical quasinormal mode approach. We show that coupling to metamaterial nano-resonators can lead to significant Purcell enhancements that are nearly an order of magnitude larger than those of plasmonic resonators with comparable geometry. However, the associated single photon output β -factors are extremely low (around 10%), far smaller than those of comparable sized metallic resonators (70%). Using a quasinormal mode expansion of the photon Green function, we describe how the low β -factors are due to increased Ohmic quenching arising from redshifted resonances, larger quality factors and stronger confinement of light within the metal. In contrast to current wisdom, these results suggest that hyperbolic metamaterial nano-structures make poor choices for single photon sources.

Introduction. Engineered cavity structures allow for tight confinement of light and the enhancement of its interaction with matter. In particular, solid state structures such as photonic crystals [1, 2], slow-light waveguides [3], plasmonic nano-structures [4–6] and metamaterial resonators [7, 8] allow for the enhancement of the photon local density of states (LDOS) of embedded quantum emitters, thereby increasing their spontaneous emission (SE) rates via the Purcell effect [9]. Such enhancement finds application in areas such as molecule sensing [10], high-resolution imaging [11, 12], energy harvesting [13, 14], nonlinear optics [15], and single photons [16].

A new class of optical materials known as hyperbolic metamaterials (HMMs) offers the possibility of achieving extreme confinement of light and increased interaction with matter over a broad spectral range [17]. Such materials consist of both metal and dielectric parts, and are typically described as having an anisotropic dielectric tensor within an effective medium description. The dielectric tensor elements ε_{\parallel} and ε_{\perp} (parallel and perpendicular to the axis of anisotropy, respectively) are of opposite sign, corresponding to metallic or dielectric properties along different axes. For an HMM that is anisotropic along the z -axis, for example, the electromagnetic dispersion relation is given by

$$\frac{k_x^2 + k_y^2}{\varepsilon_{\parallel}} + \frac{k_z^2}{\varepsilon_{\perp}} = \frac{\omega^2}{c^2}, \quad (1)$$

where \mathbf{k} is the wavevector, ω is the angular frequency, and c is the speed of light. Since ε_{\parallel} and ε_{\perp} are of opposite sign, surfaces of constant frequency are hyperbolic, extending to very large values of k . The resulting momentum mismatch between HMM and free-space electromagnetic fields results in strong confinement of light around the structure [18]. Moreover, the isofrequency dispersion implies that dipole emitters can couple to a large range of k -states at a single frequency, thereby increasing the number of possible decay paths and thus the SE rate [17].

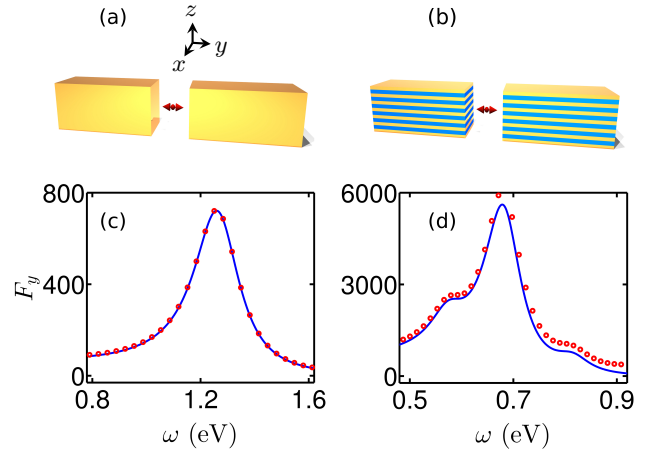


FIG. 1: (a) Schematic of a gold nano-dimer. Each parallelepiped is 95 nm in length, and 35 nm in depth and width; the gap size is 20 nm. A y -polarized quantum dipole is shown in the gap centre. (b) Schematic of an HMM dimer with 7 layers of gold and 6 layers of dielectric (blue), with layers stacked in the z -direction. (c) Purcell factor for a y -polarized dipole in the gap centre of a gold nano-dimer. Full dipole results are shown with red circles, and the result of a single QNM expansion is shown in solid blue. (d) y -projected Purcell factor in the gap centre for an HMM dimer of metal filling fraction $f_m = 0.2$, shown with the result of a full dipole calculation and with an expansion of 3 QNMs.

Metamaterial waveguides have also been shown to provide enhanced Purcell factors and Lamb shifts through the associated slow light modes [3].

It has been suggested that one of the first applications of HMM nanophotonics will be single photon sources, because of their broadband SE enhancement and tunability [17]. Indeed, it was shown in Ref. 17 that infinite multi-layered HMM structures can couple to photon emitters with a high quantum yield, suggesting the possibility of achieving high single photon output β -factors

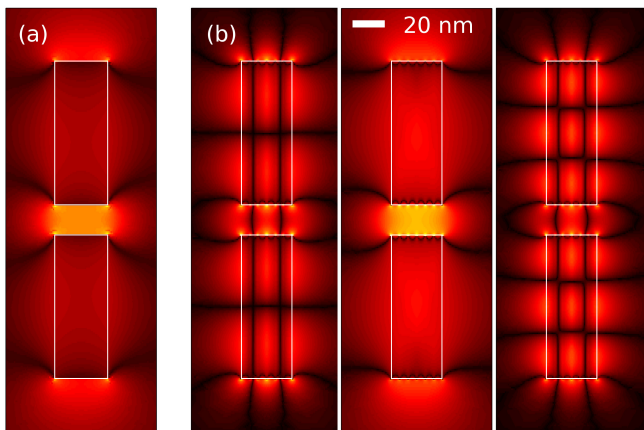


FIG. 2: (a) QNM profile $|\tilde{\mathbf{f}}_y(0, y, z)|$ for the dominant mode of a plasmonic dimer. The edges of the dimer are shown in white. (b) QNM profile for the three dominant modes of an HMM dimer with filling fraction $f_m = 0.2$, with eigenfrequencies increasing from left to right. Brighter colours indicate stronger fields.

(defined here as the probability of emitting a photon via radiative decay; along with the Purcell factor, it is the main figure of merit for an ideal single photon source). It has also been suggested that the method of light confinement in HMM cavity structures is fundamentally different from the localized surface plasmons of metals, being electro-dynamical rather than electrostatic in nature [19]. This electro-dynamical confinement, it has been argued, may reduce Ohmic dissipation and increase quality factors compared to metallic structures, implying that HMMs are better single photon candidates than plasmonic resonators. However, the Purcell enhancements reported for infinite HMM structures are orders of magnitude smaller than those of HMM nano-resonators [19], and it is not clear whether such large radiative coupling is also present in miniaturized cavity systems. It is also not clear whether larger quality factors in HMM cavity structures are necessarily associated with larger β -factors. Experimental studies are expected to provide little insight into this question, since it has been assumed that most of the emitter decay paths are into high- k states, which are difficult to observe directly in the near-field [17]. An analytical description of radiative and non-radiative decay in HMM resonators is thus of great interest.

In this Letter we study HMM nano-structures using a semi-analytical Green function approach, and compare the associated SE enhancements and β -factors with those of plasmonic resonators. We first show that the Green function of a complex, multi-layered HMM resonator can be simply and accurately described in terms of its quasi-normal modes (QNMs), the optical modes for an open dissipative cavity structure [20, 21]. We report greatly enhanced SE rates, up to an order of magnitude greater

than those of metal resonators with comparable geometry. Surprisingly however, we show that in all cases, the output β -factors are significantly lower than those of plasmonic structures, decreasing monotonically with the dielectric character of the resonator. Using a QNM approach, we show that this increased quenching is due to a combination of redshifted resonances, larger quality factors, and stronger confinement of light within the metal regions. We conclude that HMM resonators are characterized by greatly enhanced Purcell factors that are always accompanied by smaller β -factors, making them poor choices for single photon sources, though they are certainly interesting for quantum optics studies.

QNM Green Function Expansion. The interaction of light with matter can be rigorously described in terms of the photon Green function. For example, the LDOS enhancement $\rho(\mathbf{r}_a, \omega)/\rho^h(\mathbf{r}_a, \omega)$ of an \mathbf{n}_a -polarized emitter at position \mathbf{r}_a is given by the ratio $\text{Im}\{\mathbf{n}_a \cdot \mathbf{G}(\mathbf{r}_a, \mathbf{r}_a; \omega) \cdot \mathbf{n}_a\} / \text{Im}\{\mathbf{n}_a \cdot \mathbf{G}^h(\mathbf{r}_a, \mathbf{r}_a; \omega) \cdot \mathbf{n}_a\}$ [22], where \mathbf{G} is the Green function and h denotes a homogeneous background medium. Within the weak to intermediate coupling regime, the LDOS enhancement represents the Purcell factor. Moreover, the Green function can be used to quantify the non-radiative decay rate, through [5, 23]

$$\gamma^{\text{nr}}(\mathbf{r}_a, \omega) = \frac{2}{\hbar\omega\epsilon_0} \int_V \text{Re}\{\mathbf{j}(\mathbf{r}) \cdot \mathbf{G}^*(\mathbf{r}, \mathbf{r}_a; \omega) \cdot \mathbf{d}_a\} d\mathbf{r}, \quad (2)$$

where $\mathbf{d}_a = d\mathbf{n}_a$ is transition dipole of the emitter, and $\mathbf{j}(\mathbf{r}) = \omega \text{Im}\{\epsilon(\mathbf{r}, \omega)\} \mathbf{G}(\mathbf{r}, \mathbf{r}_a; \omega) \cdot \mathbf{d}_a$ is the induced current density within the scattering geometry.

The Green function is known analytically in a few simple cases, but in general must be obtained numerically. Full numerical dipole simulations can yield the Green function $\mathbf{G}(\mathbf{r}, \mathbf{r}_a; \omega)$ at the dipole location \mathbf{r}_a [4, 24, 25], but require another lengthy simulation to quantify the relevant physics at each new position. Instead, the Green function may be expanded in terms of the QNMs of the scattering geometry. The QNMs $\tilde{\mathbf{f}}_\mu$ are the source-free solution to Maxwell's equations with open boundary conditions [26, 27], with a discrete set of complex eigenvalues $\tilde{\omega}_\mu = \omega_\mu - i\gamma_\mu$, and associated quality factors $Q = \omega_\mu/2\gamma_\mu$. Due to the outgoing boundary conditions, QNMs diverge (exponentially) in space [26, 28], but their norm is still finite, and can be obtained in a number of equivalent ways (e.g. [29–31]). Within the resonator of interest [26], the transverse part of the electromagnetic Green tensor can be written as an expansion of its QNMs, through [27] $\mathbf{G}^T(\mathbf{r}, \mathbf{r}'; \omega) = \sum_\mu (\omega^2/2\tilde{\omega}_\mu(\tilde{\omega}_\mu - \omega)) \tilde{\mathbf{f}}_\mu(\mathbf{r}) \tilde{\mathbf{f}}_\mu^T(\mathbf{r}')$. For positions near metallic resonators (but outside the regime of quasi-static quenching), the Green function can be accurately approximated by the same expansion [32], with the sum greatly reduced to the contribution of one or a few dominant modes near the main cavity resonance

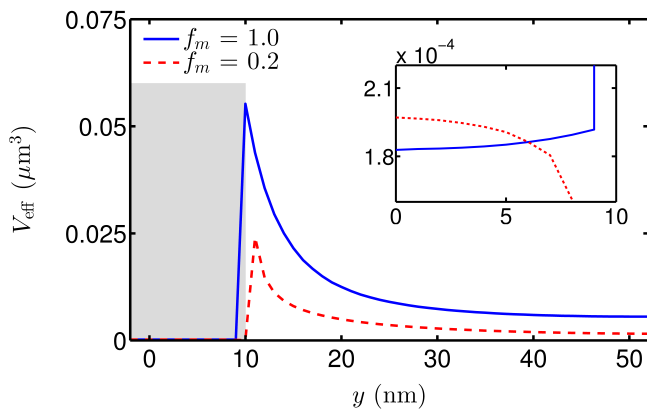


FIG. 3: Effective mode volume, $V_{\text{eff}}(0, y, 0)$, for the dominant modes of the plasmonic dimer (solid blue) and HMM dimer (dashed red). Note that $x = z = 0$ and $y > 10$ nm corresponds to positions inside a metal layer of the HMM dimer, and $y < 10$ nm (shaded region) corresponds to positions outside the resonator. Inset: zoom-in of the effective mode volume for positions outside the resonator, $y = 0$ to $y = 10$ nm. The inflection point in the HMM mode volume (not shown) corresponds to a field hot spot near the edge of the metal layer.

[21]. Thus obtaining the dominant QNMs is usually sufficient for obtaining the Green function as a function of frequency and position around the resonator. The Green function and QNMs can then be used in various quantum optics formalisms [2, 23, 33], providing the starting point for an analytical and rigorous description of light-matter interactions.

HMM Nano-Dimers. For practical purposes we analyze a parallelepiped nano-scale HMM dimer with 7 layers of gold and 6 layers of dielectric, anisotropic along the z -axis (Fig. 1b), but our general findings below apply to all HMM geometries that we have tried (more details are given below). The dimer configuration enhances Purcell factors in the gap through the bonding effect, and minimizes non-radiative quenching by drawing fields out of the metal [34]. The length of each parallelepiped is 95 nm (y -axis), and the width and depth are 35 nm (x - and z -axes). We set the gap size to 20 nm in order to maximize the Purcell factor while minimizing non-radiative quenching. The resonator is characterized as a type-II HMM, since its permittivity tensor is metallic along two axes, and dielectric along the third. We set $\varepsilon = 2.9$ for the dielectric (similar to MgO) and $\varepsilon^h = 2.25$, and use a Drude model for gold, $\varepsilon(\omega) = 1 - \omega_p^2/(\omega(\omega + i\gamma))$. We set the plasmon frequency $\omega_p = 1.202 \times 10^{16}$ rad/s and collision rate $\gamma = 1.245 \times 10^{14}$ rad/s, with parameters obtained by fitting experimental data for gold in the frequency regime of interest [35].

We obtain the QNMs around the resonance of interest for two representative cases: a plasmonic resonator (volume metal filling fraction $f_m = 1.0$), and an HMM resonator with large dielectric character ($f_m = 0.2$).

Using COMSOL Multiphysics [36], we use an iterative frequency-domain pole search with a dipole excitation [37] to obtain the complex eigenfrequencies, and the associated modes are normalized implicitly. We identify a single complex eigenfrequency for the pure gold dimer, $\tilde{\omega}_c/2\pi = 303.29 - i24.18$ THz ($Q = 6.3$). We obtain a maximum Purcell factor of around 720 at the origin (gap centre), in excellent agreement with full dipole calculations (Fig. 1c). The HMM dimer response is characterized by three complex eigenfrequencies contributing to the resonance of interest, $\tilde{\omega}_{c_1}/2\pi = 139.215 - i9.847$ THz ($Q = 7.1$), $\tilde{\omega}_{c_2}/2\pi = 165.335 - i10.412$ THz ($Q = 7.9$), and $\tilde{\omega}_{c_3}/2\pi = 197.472 - i9.860$ THz ($Q = 10.0$). The three-sum QNM maximum Purcell factor at the origin is approximately 5600, which is within 5% of the full dipole result of 5900 (Fig. 1d; the presence of other nearby modes makes the expansion slightly less accurate than that of the gold dimer). The HMM and gold QNM profiles are shown in Fig. 2; we remark that the dominant contribution at the origin is from the second QNM, which resembles a plasmonic mode; in contrast, modes 1 and 3 resemble Fabry-Pérot resonances, and contribute strongly at other locations.

Clearly the Purcell factors achievable with the HMM are much higher than those of the pure gold structure (in this case, by an order of magnitude). Moreover, the quality factor is enhanced and the metal volume is diminished, suggesting that the HMM dimer may be associated with less Ohmic loss. However, full dipole calculations yield an impressive β -factor of up to 72% for the metallic resonator, but an extremely poor β -factor of 12% for the HMM. We have found similarly low β -factors for different geometries and configurations, including HMM waveguides, and cylindrical nano-rods and dimers (type-I HMMs). The fundamental results were unchanged when modelling the structures as effective homogeneous media. We have also found low β -factors in the high- Q HMM sphere studied in Ref. 19; while the authors suggested high radiation quality factors as evidence of decreased energy loss in HMM resonators, we found that the β -factors were under 6% in all high-Purcell regions. To our knowledge, this is the first time that such large losses have been documented in such a wide variety of HMM resonators, and our results stand in contrast to current suggestions in the literature.

QNM Description of Large Losses. We argue below that the universally low single photon β -factors associated with HMMs are attributable to three key factors: (a) HMMs confine light to their metal regions more strongly than metallic resonators, (b) HMM modes have higher quality factors than plasmonic modes, and (c) HMM resonances are redshifted to regimes of higher metallic loss as the metal filling fraction is reduced. In order to understand the first two points, we consider Eq. (2) for the case of a y -polarized dipole at \mathbf{r}_a . Focusing on a single QNM of interest, the total decay rate is

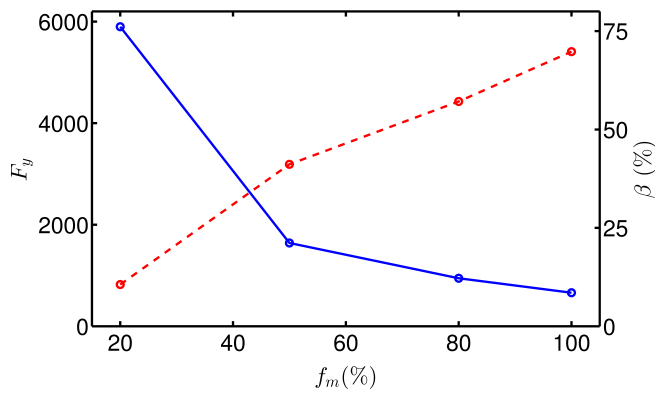


FIG. 4: Mid-gap on-resonance Purcell factor (solid blue) and output β -factor (dashed red) for a y -polarized dipole at the origin for varying filling fractions. Clearly, an increase in the Purcell factor is always accompanied by a reduction in the β -factor.

proportional to $\text{Im}\{G_{yy}(\mathbf{r}_a, \mathbf{r}_a; \omega)\} = \text{Im}\{A(\omega)f_y^2(\mathbf{r}_a)\}$, where we have defined $A(\omega) = \omega^2/2\tilde{\omega}_c(\tilde{\omega}_c - \omega)$ for the c^{th} QNM, and where we have withheld the c -dependence of the mode for ease of notation. On the other hand, the non-radiative decay rate given by Eq. (2) scales with $\varepsilon_I |A(\omega)|^2 |\tilde{f}_y(\mathbf{r}_a)|^2 \int_{\text{metal}} |\tilde{\mathbf{f}}(\mathbf{r})|^2 d\mathbf{r}$, where $\varepsilon_I = \text{Im}\{\varepsilon\}$, and where we have used vertical bars to indicate both an absolute value and the norm of a vector. For $(\text{Im}\{\tilde{f}\}/\text{Re}\{\tilde{f}\})^2 \ll 1$ and $\text{Im}\{\tilde{f}\}/\text{Re}\{\tilde{f}\} \ll Q$, both of which are almost always satisfied in practice, the on-resonance non-radiative coupling $\eta^{\text{nr}} = \gamma^{\text{nr}}/\gamma$ is given by

$$\eta^{\text{nr}} \propto f_m \varepsilon_I Q \langle 1/V_{\text{eff}} \rangle_{\text{metal}}, \quad (3)$$

where $\langle \dots \rangle_{\text{metal}}$ denotes a spatial averaging over the metallic volume, V_{eff} is the effective mode volume, defined via [38] $1/V_{\text{eff}}(\mathbf{r}) = \text{Re}\{\varepsilon^h \tilde{\mathbf{f}}(\mathbf{r}) \cdot \tilde{\mathbf{f}}(\mathbf{r}) / \langle \tilde{\mathbf{f}} | \tilde{\mathbf{f}} \rangle\}$, and we have expressed the integration volume as $V_{\text{metal}} = f_m V_{\text{dimer}}$. The effective mode volume here is not the usual measure of the space occupied by the resonant mode; rather, it is a convenient measure of local light confinement for use in Purcell's original formula, $F \propto Q/V$ [21]. Note also that the non-radiative decay rate scales with G^2 , while the total decay rate scales with G , so that the non-radiative coupling is increased by an enhancement of Q/V_{eff} within the metal even if Q/V_{eff} increases at \mathbf{r}_a as well.

Figure 3 shows $V_{\text{eff}}(0, y, 0)$ as a function of distance y along the dimer axis, for both $f_m = 1.0$ and $f_m = 0.2$. In the metallic region of the dimer ($y > 10$ nm), the effective mode volume of the HMM is significantly smaller than that of the gold dimer, which, in light of the above discussion, suggests a much-reduced β -factor. However, for positions outside the resonator ($y < 10$ nm, inset of Fig. 3) the effective mode volume is almost identical in each case (it is, in fact, slightly smaller for the gold dimer). This suggests that the HMM is not characterized by a smaller effective mode volume at all positions,

which would simultaneously increase the Purcell factor while diminishing the β -factor (see *Comments* below). In fact, the increased confinement of light occurs only within the metal. We can understand this effect as arising from the increased overlap between metal and dielectric within the resonator. Since the dielectric supports the existence of electric fields better than the metal, the presence of more overlapping dielectric allows the fields to leak into the metal, thereby increasing loss. Such an explanation would suggest that smaller metal filling fractions are associated with higher loss, which is indeed observed (Fig. 4). Since the mode volume is reduced only within the metal, and since this reduction scales with the dielectric character of the resonator, we suggest that this effect is characteristic of all resonators consisting of metal and dielectric layers, and is indeed consistent with all cases we have studied.

The β -factor is further reduced by an increase in quality factor, $Q^{\text{HMM}}/Q^{\text{metal}} = 1.27$, and from the redshifting of the resonance frequency, since metals with a Drude-like dispersion are characterized by a loss term $\varepsilon_I \propto 1/\omega^3$. Importantly, this latter effect balances the reduction in the metal volume, such that $f_m \varepsilon_I = 3.16$ on resonance for the HMM dimer, while the same product is equal to 2.59 for the gold dimer. This balancing effect, combined with increased Q -factors and enhanced light confinement within the metal, leads to lower β -factors associated with the HMM dimer.

In light of the above results, we suggest that HMM resonators make poor single photon sources, for any Purcell factor improvement over metal resonators is accompanied by a reduction in the β -factor (which renders the photon source increasingly non-deterministic). This surprising result is expected to be true of all forms of HMM nano-resonators, given the general form of the explanation given above, and we have found it to be true in all the examples we have studied.

Comments. While low β -factors make HMM resonators poor choices for single photon sources, the large accompanying Purcell enhancements would seem to suggest access to non-perturbative quantum optics effects such as the strong coupling regime and vacuum Rabi splitting. Such applications requires a large Green function and quality factor [22]. However, the extreme enhancement of the Purcell factor is due in large part to the redshifting of the resonance frequency, and not due to a significant enhancement of the magnitude of the Green function. Since the free-space decay rate of a dipole emitter scales with ω^3 [22], the redshift of the resonance from 303.3 to 165.3 THz decreases the free-space decay rate by a factor of 6.2. This redshift, combined with a relatively modest quality factor increase from $Q = 6.3$ to $Q = 7.9$, yields a 7.8-fold enhancement in the Purcell factor, which is almost identical to the value obtained with the QNM expansion. The enhancement of the Green function is therefore quite minor, making it unlikely for strong coupling to be achieved

in HMMs if it cannot already be achieved in metallic resonators. Indeed, we have found that vacuum Rabi splitting for a typical quantum dot dipole requires Purcell factors that are orders of magnitude larger than any of the enhancements found here. However, the strong resonance redshifting associated with modified filling fractions provides an important opportunity to finely tune to dipole resonances, which is of great interest experimentally.

Conclusions. We have shown that coupling to HMM nano-resonators can lead to Purcell enhancements that are much larger than those of metals with comparable geometries. Surprisingly, however, we have found that these enhancements are associated with unusually low β -factors. Using a semi-analytical QNM approach, we have shown that these low β -factors are due to redshifted resonances, increased quality factors and stronger confinement of light within the metal. We conclude that HMM nano-resonators are poor choices for single photon sources and other applications requiring strong radiative coupling; however, they offer an important opportunity to finely-tune to dipole resonances by varying the metal character of the resonator, and facilitate important fundamental studies in plasmonic quantum optics.

Acknowledgements

This work was supported by the Natural Sciences and Engineering Research Council of Canada. We would like to acknowledge CMC Microsystems for the provision of COMSOL Multiphysics to facilitate this research, and we thank Rongchun Ge for useful discussions.

* Electronic address: shughes@queensu.ca

- [1] P. Lodahl, A. F. Van Driel, I. S. Nikolaev, A. Irman, K. Overgaag, D. Vanmaekelbergh, and W. L. Vos, *Nature* **430**, 654 (2004).
- [2] S. Hughes, *Opt. Lett.* **29**, 2659 (2004).
- [3] P. Yao, C. Van Vlack, A. Reza, M. Patterson, M. M. Dignam, and S. Hughes, *Phys. Rev. B* **80**, 195106 (2009).
- [4] P. Yao, V. S. C. Manga Rao, and S. Hughes, *Laser Photonics Rev.* **4**, 499 (2010).
- [5] P. Anger, P. Bharadwaj, and L. Novotny, *Phys. Rev. Lett.* **96**, 113002 (2006).
- [6] M. Frimmer and A. F. Koenderink, *Phys. Rev. Lett.* **110**, 217405 (2013).
- [7] Z. Jacob, J.-Y. Kim, G.V. Naik, A. Boltasseva, E. E. Narimanov, and V. M. Shalaev, *Appl. Phys. B* **100**, 215 (2010).
- [8] M. A. Noginov, H. Li, Y. A. Barnakov, D. Dryden, G. Nataraj, G. Zhu, C. E. Bonner, M. Mayy, Z. Jacob, and E. E. Narimanov, *Opt. Lett.* **35**, 1863 (2010).
- [9] E. M. Purcell, *Phys. Rev.* **69**, 37 (1946).
- [10] J. Homola, S. S. Yee, and G. Gauglitz, *Sens. Actuators B* **54**, 3 (1999).
- [11] K. Kneipp, Y. Wang, H. Kneipp, L. T. Perelman, I. Itzkan, R. R. Dasari, and M. S. Feld, *Phys. Rev. Lett.* **78**, 1667 (1997).
- [12] R. Zhang, Y. Zhang, Z. C. Dong, S. Jiang, C. Zhang, L. G. Chen, L. Zhang, Y. Liao, J. Aizpurua, Y. E. Luo, J. L. Yang, and J. G. Hou, *Nature* **498**, 82 (2013).
- [13] H. A. Atwater and A. Polman, *Nat. Mater.* **9**, 205 (2010).
- [14] Z. Yu, A. Raman, and S. Fan, *Proc. Natl. Acad. Sci. U.S.A.* **107**, 17491 (2010).
- [15] M. Kauranen and A. V. Zayats, *Nat. Photon.* **6**, 737 (2012).
- [16] D. E. Chang, A. S. Sørensen, E. A. Demler, and M. D. Lukin, *Nat. Phys.* **3**, 11 (2007).
- [17] C. L. Cortes, W. Newman, S. Molesky, and Z. Jacob, *J. Opt.* **14**, 063001 (2012).
- [18] X. Yang, J. Yao, J. Rho, X. Yin, and X. Zhang, *Nat. Photon.* **6**, 450 (2012).
- [19] C. Wu, A. Salandrino, X. Ni, and X. Zhang, *Phys. Rev. X* **4**, 021015 (2014).
- [20] E. S. C. Ching, P. T. Leung, A. M. van den Brink, W. M. Suen, S. S. Tong, and K. Young, *Rev. Mod. Phys.* **70**, 1545 (1998).
- [21] P. T. Kristensen and S. Hughes, *ACS Photonics* **1**, 2 (2014).
- [22] L. Novotny and B. Hecht, *Principles of Nano-Optics* (Cambridge University Press, Cambridge, England, 2006).
- [23] R.-C. Ge and S. Hughes, *Phys. Rev. B* **92**, 205420 (2015).
- [24] C. Van Vlack and S. Hughes, *Opt. Lett.* **37**, 2880 (2012).
- [25] V. S. C. Manga Rao and S. Hughes, *Phys. Rev. Lett.* **99**, 193901 (2007).
- [26] P. T. Leung, S. Y. Liu, and K. Young, *Phys. Rev. A* **49**, 3982 (1994).
- [27] K. M. Lee, P. T. Leung, and K. M. Pang, *J. Opt. Soc. Am. B* **16**, 1409 (1999).
- [28] J. U. Nökel and R. K. Chang 2002 in *Cavity-Enhanced Spectroscopies* ed R. D. van Zee and J. P. Looney (San Diego, CA: Academic).
- [29] H. M. Lai, P. T. Leung, K. Young, P. W. Barber, and S. C. Hill, *Phys. Rev. A* **41**, 5187 (1990).
- [30] C. Sauvan, J. P. Hugonin, I. S. Maksymov, and P. Lalanne, *Phys. Rev. Lett.* **110**, 237401 (2013).
- [31] P. T. Kristensen, R.-C. Ge, and S. Hughes, *Phys. Rev. A* **92**, 053810 (2015).
- [32] R.-C. Ge, P. T. Kristensen, J. F. Young, and S. Hughes, *New J. Phys.* **16**, 113048 (2014)
- [33] C. Van Vlack, P. T. Kristensen, and S. Hughes, *Phys. Rev. B* **85**, 075303 (2012).
- [34] R.-C. Ge and S. Hughes, *Opt. Lett.* **39**, 4235 (2014).
- [35] P. B. Johnson and R. W. Christy, *Phys. Rev. B* **6**, 4370 (1972).
- [36] COMSOL Multiphysics: www.comsol.com.
- [37] Q. Bai, M. Perrin, C. Sauvan, J. P. Hugonin, and P. Lalanne, *Opt. Expr.* **21**, 27371 (2013).
- [38] P. T. Kristensen, C. Van Vlack, and S. Hughes, *Opt. Lett.* **37**, 1649 (2012).